Effect of Ligands on HP-Induced Unfolding and Oligomerization of β-Lactoglobulin

Simeon Minić, Burkhard Annighöfer, Arnaud Hélary, Djemel Hamdane, Gaston Hui Bon Hoa, Camille Loupiac, Annie Brûlet, Sophie Combet

Dear author,

Please note that changes made in the online proofing system will be added to the article before publication but are not reflected in this PDF.

We also ask that this file not be used for submitting corrections.

Please cite this article in press as: Minić et al., Effect of Ligands on HP-Induced Unfolding and Oligomerization of β-Lactoglobulin, Biophysical Journal (2020), https://doi.org/10.1016/j.bpj.2020.10.019

Biophysical *Journal*
Article

Biophysical Society

Effect of Ligands on HP-Induced Unfolding and Oligomerization of β-Lactoglobulin

Simeon Minić,[1,*] Burkhard Annighöfer,[1] Arnaud Hélary,[1] Djemel Hamdane,[2] Gaston Hui Bon Hoa,[3] Camille Loupiac,[4] Annie Brûlet,[1] and Sophie Combet[1,*]

[1]Université Paris-Saclay, Laboratoire Léon-Brillouin, UMR12 CEA-CNRS, CEA-Saclay, Gif-sur-Yvette CEDEX, France; [2]Laboratoire de Chimie des Processus Biologiques, CNRS-UMR 8229, Collège de France, Paris CEDEX 05, France; [3]National Institute of Health and Medical Research (INSERM), Paris, France; and [4]Université de Bourgogne Franche-Comté, AgroSup Dijon, UMRA 02.102 Procédés Alimentaires et Microbiologiques, Equipe Physico-Chimie des Aliments et du Vin, Dijon, France

ABSTRACT To probe intermediate states during unfolding and oligomerization of proteins remains a major challenge. High pressure (HP) is a powerful tool for studying these problems, revealing subtle structural changes in proteins not accessible by other means of denaturation. Bovine β-lactoglobulin (BLG), the main whey protein, has a strong propensity to bind various bioactive molecules such as retinol and resveratrol, two ligands with different affinity and binding sites. By combining in situ HP-small-angle neutron scattering (SANS) and HP-ultraviolet/visible absorption spectroscopy, we report the specific effects of these ligands on three-dimensional conformational and local changes in BLG induced by HP. Depending on BLG concentration, two different unfolding mechanisms are observed in situ under pressures up to ∼300 MPa: either a complete protein unfolding, from native dimers to Gaussian chains, or a partial unfolding with oligomerization in tetramers mediated by disulfide bridges. Retinol, which has a high affinity for the BLG hydrophobic cavity, significantly stabilizes BLG both in three-dimensional and local environments by shifting the onset of protein unfolding by ∼100 MPa. Increasing temperature from 30 to 37°C enhances the hydrophobic stabilization effects of retinol. In contrast, resveratrol, which has a low binding affinity for site(s) on the surface of the BLG, does not induce any significant effect on the structural changes of BLG due to pressure. HP treatment back and forth up to ∼300 MPa causes irreversible covalent oligomerization of BLG. Ab initio modeling of SANS shows that the oligomers formed from the BLG-retinol complex are smaller and more elongated compared to BLG without ligand or in the presence of resveratrol. By combining HP-SANS and HP-ultraviolet/visible absorption spectroscopy, our strategy highlights the crucial role of BLG hydrophobic cavity and opens up new possibilities for the structural determination of HP-induced protein folding intermediates and irreversible oligomerization.

SIGNIFICANCE High pressure (HP) is a powerful probe to access the intermediate states of proteins through subtle structural changes not accessible by other means of denaturation. Bovine β-lactoglobulin (BLG), the main whey protein, is able to bind various bioactive molecules, such as retinol and resveratrol, exhibiting different affinity and binding sites. By combining HP-small-angle neutron scattering and HP-ultraviolet/visible absorption spectroscopy, we highlight two different mechanisms during the unfolding and oligomerization of BLG depending on protein concentration. Above all, we show that retinol significantly prevents the unfolding and oligomerization of BLG, unlike resveratrol, emphasizing the crucial role of the hydrophobic cavity in BLG stabilization. Our strategy opens up new possibilities for the structural determination of protein intermediates and oligomers using HP.

INTRODUCTION

The understanding of protein folding, misfolding, and unfolding remains a major challenge in structural biology. High pressure (HP) is a powerful tool to probe the mechanisms of protein folding by elucidating the dynamics and structure of folding intermediates (1). Nowadays, it is very well known that the use of HP results in the disruption of the native structure of proteins because of the decrease of the volume of the protein-solvent complex upon denaturation. HP studies thus provide a fundamental thermodynamic parameter for protein unfolding, i.e., the volume change (2). Recent studies demonstrate that pressure mostly unfolds proteins through hydrophobic cavities present in the

Submitted June 29, 2020, and accepted for publication October 19, 2020.

*Correspondence: simeonminic@yahoo.com or sophie.combet@cea.fr

Editor: Jill Trewhella.

https://doi.org/10.1016/j.bpj.2020.10.019

Please cite this article in press as: Minić et al., Effect of Ligands on HP-Induced Unfolding and Oligomerization of β-Lactoglobulin, Biophysical Journal (2020), https://doi.org/10.1016/j.bpj.2020.10.019

folded state that are eliminated in the unfolded states (3). Internal cavities are thus important structural features for proteins and sources of fluctuation between different conformational states, which can be stabilized by subsequent ligand binding.

Bovine β-lactoglobulin (BLG), the main whey protein of cow milk, belongs to the lipocalin protein family, whose members fold up into eight-stranded antiparallel β-barrels arranged to form the central hydrophobic cavity (Fig. 1; (6)). An intramolecular disulfide bridge between cysteins (Cys) 106 and 119 stabilizes this β-barrel structure (Fig. 1). Additionally, Cys66 and Cys160 residues form the second disulfide bond, close to the edge of the hydrophobic cavity (7), whereas Cys121 exists in free form and is buried under an α-helix located on the surface of the native protein (Fig. 1; (8)). The presence of a hydrophobic cavity gives BLG the ability to bind reversibly with high affinity various hydrophobic ligands such as retinol (vitamin A, owning a mostly hydrophobic tail), other fatty acids, cholesterol, vitamin D, etc. (6). In contrast, other ligands such as bioactive polyphenol resveratrol (9) and protoporphyrin IX (10), which are much less hydrophobic, can bind surface site(s) of BLG but with a lower affinity. In our study, we focus on retinol and resveratrol, two BLG ligands exhibiting 1) different BLG binding sites (Fig. 1); 2) high or low affinity, with K_a of 10^8 and 10^4 L/mol for retinol and resveratrol, respectively (6,9); and 3) a bit higher solubility at pH 7 for resveratrol than for retinol.

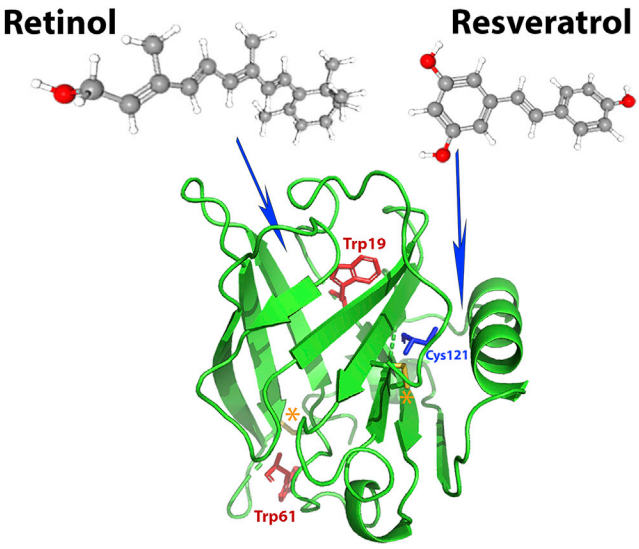

Web 3C

FIGURE 1 Ribbon model of the crystal structure of BLG monomer (3BLG.pdb). Arrows indicate retinol (4) and resveratrol (5) approximative binding sites. Tryptophan (Trp) aromatic side chains are shown in red (Trp19 and Trp61), with Trp19 residue close to the BLG cavity. The free cystein Cys121, colored in blue, is not accessible in the native folded state of BLG but is exposed to the solvent after protein unfolding. The disulfide bridges are colored in orange and marked with an asterisk (*). Both retinol and resveratrol ligands are not to scale. To see this figure in color, go online.

BLG behavior at HP conditions has been extensively studied by numerous techniques, such as ultraviolet/visible (UV/vis) absorption (11), fluorescence (12), and Fourier-transform infrared spectroscopy (13), as well as two-dimensional NMR (14) and small-angle x-ray or neutron scattering (SAXS or SANS, respectively) (13,15). BLG exists in the native state as a monomer at pH 2 and a dimer at neutral pH (16). Because of its hydrophobic cavity, BLG is very sensitive to pressure denaturation and therefore constitutes an adequate model to study HP protein unfolding. It unfolds at pressures between 100 and 200 MPa (13), but the pressure stability of the protein strongly depends on its solvent pH, the protein being more stable at pH 2 than at neutral pH (12). It is well known that ligand binding can prevent the thermal denaturation of proteins (17). However, the effect of ligands on the pressure-dependent structural changes of proteins has not been thoroughly studied compared to thermal or chemical denaturation. From a fundamental point of view, BLG therefore represents a relevant and sensitive model system to study the effect of ligand binding on protein stability, folding, and self-association (18) under HP conditions. BLG is able to form noncovalent oligomers, and such an oligomerization strongly depends on pH and ionic strength (16). An increased population of unfolded BLG molecules can also promote amyloid fibril formation (19).

In this study, we compare the effects of retinol and resveratrol ligands on HP-dependent stability of BLG. We measured both in situ HP-SANS, to study the tridimensional conformational changes, and in situ HP-UV/vis absorption, to follow the changes in the local environment of aromatic amino acid residues (tryptophan (Trp) residues, especially) (Fig. 1). We report that retinol strongly reduces HP-induced large conformational changes on BLG, whereas resveratrol binding does not produce any significant changes. HP treatment back and forth up to ~300 MPa causes irreversible BLG covalent oligomerization while keeping "molten globule" folded conformations. The high-affinity binding of retinol in BLG hydrophobic cavity prevents such protein oligomerization, in contrast to resveratrol.

MATERIALS AND METHODS

Materials

BLG was purified as previously described by Fox et al. (20). Protein concentration was determined spectrophotometrically using the extinction coefficient of 17,600 M^{-1} cm^{-1} at 278 nm (21). BLG was dialyzed against 50 mM Tris buffer in D_2O (pD 7.2) or 100 mM Tris buffer in H_2O (pH 7.2) for HP-SANS and HP-UV/vis measurements, respectively.

Ligands were purchased from Sigma-Aldrich (St. Louis, MO). Retinol and resveratrol were solubilized in deuterated ethanol (d6; Sigma-Aldrich) with a concentration not exceeding 2% (v/v). Addition of 2% d-ethanol is the minimal ethanol concentration necessary to solubilize the retinol and resveratrol ligands. The stoichiometry of both ligands is stated to be 1:1 protein/ligand molar ratio (5). In SANS measurements, because of very low solubility, the hydrophobic retinol ligand was used at only 5 mg/mL,

Please cite this article in press as: Minić et al., Effect of Ligands on HP-Induced Unfolding and Oligomerization of β-Lactoglobulin, Biophysical Journal (2020), https://doi.org/10.1016/j.bpj.2020.10.019

whereas resveratrol was solubilized at 8 mg/mL. All measurements were performed at 30°C, unless otherwise stated, and at pH/pD 7.2 to enhance ligand solubility, especially for retinol. Fully chemical unfolding of BLG was performed by dissolving the protein in D_2O solution of 6 M deuterated guanidine in DCl (Sigma-Aldrich) at pD adjusted to 7.2. All other chemicals were of analytical reagent grade, and milli-Q water was used as solvent.

SDS-PAGE

Sodium dodecyl sulfate-polyacrylamide gel electrophoresis (SDS-PAGE) of BLG in the absence or presence of ligands, before and after HP-SANS measurements, was performed under nonreducing conditions (22), unless it is otherwise stated. An amount of 12 μg of each protein sample was applied on 4–20% gradient precast gel (Bio-Rad Laboratories, Hercules, CA). Gels were stained using Coomassie brilliant blue G-250 (Sigma-Aldrich), and band intensities were quantitated using ImageJ software (National Institutes of Health, Bethesda, MD). The intensity of each band was normalized to the total band intensity within sample, and results were expressed as percentage.

HP-UV/visible absorption spectroscopy

UV/vis absorption spectra under in situ HP were recorded on a Cary 3E spectrometer (Varian, Palo Alto, CA) using an HP optical bomb with sapphire windows and HP generator as previously described (23). A square quartz cell (with an optical pathlength of 5 mm) containing the sample was positioned within HP optical bomb, and a plastic membrane on the top of the cell separated the sample from the pressure-transmitting liquid (H_2O). Absorbance of BLG solution (100 μM or 2 mg/mL) in the presence or the absence of 100 μM ligand (retinol or resveratrol) was recorded between 250 and 310 nm, with a bandwidth of 1 nm and a data interval of 0.1 nm, at a scanning speed of 30 nm/min. Spectra were recorded at various pressures (between 0.1 to 300 MPa, with steps of 20 or 30 MPa) at 30 or 37°C. The pressure was increased at a speed of 10 MPa/min. Measurements of buffer solutions in the absence or presence of ligands (without protein) were performed at the same conditions as above, and recorded spectra were subtracted from the spectra of BLG without ligand or BLG-ligand complexes, respectively. The fourth derivative spectra were calculated by OriginPro 8.5 Software using the Savitzky-Golay smoothing algorithm with 100-point window. The exact position of the maximal absorption bands at ~291 nm (characteristic of Trp residues of BLG) in the fourth derivative spectra was determined, and the percentage of protein unfolding was determined using the following equation:

$$\%_{BLG\ unfolding} = \frac{\lambda_{0.1\ MPa} - \lambda_P}{\lambda_{0.1\ MPa} - \lambda_{300\ MPa}} \times 100, \qquad (1)$$

where $\lambda_{0.1\ MPa}$, $\lambda_{300\ MPa}$, and λ_P represent the absorption maximum at 0.1, 300 MPa, and a given pressure, respectively. Absorption at 300 MPa is used as a reference of unfolded BLG protein, as shown by Dufour et al. (12). The results were expressed as the percentage of unfolded BLG as a function of pressure. The Gibbs free energy ($\Delta G_{0.1\ MPa}$ at 0.1 MPa) and the apparent volume change of unfolding (ΔV_u) were determined by fitting the pressure denaturation curves with the following equation adapted from (24) by replacing the A_l and A_h amplitudes by 0 and 100, respectively:

$$\%_{BLG\ unfolding} = 100 - \frac{100}{1 + e^{-\frac{\Delta G_{0.1\ MPa} + \Delta V_u \times P}{RT}}}. \qquad (2)$$

The pressure value at which one half of proteins is unfolded (50%) represents the half-denaturation pressure ($P_{1/2}$) of BLG.

HP-SANS measurements

SANS measurements were performed on PACE SANS instrument at the Laboratoire Léon-Brillouin (LLB, Saclay, France). HP-SANS experiments were performed using a new HP-SANS cell developed at LLB (25), using two metallic TiAl6V4 ELI windows (3 mm thickness each) and a sample pathlength of 4.6 mm. HP-SANS spectra were recorded at 5, 100, 150, 200, 250, and 300 MPa. The scattering signals of empty HP cell, empty beam, and electronic noise were also recorded to be able to extract the scattering signal from BLG solutions despite the large scattering signal coming from the empty HP cell (Fig. S1; (26)). Each BLG sample was measured in a quartz Hellma cell (with a pathlength of 2 mm; Hellma, Müllheim, Germany) before and after HP treatment. For measurements in the quartz cell, the Q-range covers 6.0 10^{-3}–0.5 $Å^{-1}$, whereas for measurements in the HP cell, because of geometrical and scattering constraints, the Q-range was limited to 2 10^{-2}–0.2 $Å^{-1}$. However, this latter Q-range is adequate to analyze BLG structural changes.

BLG-retinol and BLG-resveratrol complexes (1:1 M ratio) were measured at protein dilute concentrations to limit aggregation, at 5 mg/mL (274 μM) or 8 mg/mL (440 μM), respectively. The reduced protein concentration of the retinol-BLG complex, because of the lower solubility of retinol compared with resveratrol, was used to avoid ligand precipitation To get a relevant control, BLG protein without ligand was measured at the same concentration containing 2% (v/v) deuterated ethanol. Such ethanol concentration has been reported to be low enough to have no significant incidence on BLG native structure (27). Pressure was increased at a rate of ~10 MPa/min. Measurements were performed at 30 or 37°C for retinol to compare with a condition with both higher ligand solubility and binding affinity. The pressure dependence for buffer SANS intensity was also checked to be negligible (data not shown). A constant background of 0.05–0.06 cm^{-1}, deduced by measuring scattering intensity in a Hellma cell at the Q-range between 0.4 and 0.5 $Å^{-1}$, was subtracted as incoherent signal from the SANS intensities of all BLG solutions under pressure.

Air bubbles, which may be introduced during the sample injection into the HP cell, were compressed by gently increasing the pressure up to 5 MPa. We checked that BLG SANS curves in the HP cell at this "ambient" pressure were mostly superimposable to the curves of the same sample measured in a Hellma cell (Fig. S1), showing that SANS curves at 5 MPa can be considered as references for native BLG.

SANS data analysis

The classical expression of the scattering intensity $I(Q)$ (in cm^{-1}) of spherically symmetric, homogenous, and relatively monodisperse particles can be written

$$I(Q) = n\,\Delta\rho^2\,V_{part.}^2\,P(Q)S(Q), \qquad (3)$$

where n is the number of particles per volume unit (cm^{-3}), $\Delta\rho$ the difference of the neutron scattering length density between the particles and the solvent (cm^{-2}), and $V_{part.}$ (cm^3) the specific volume of the particles.

The form factor $P(Q)$ describes the shape of the particles and fulfills the condition $P(0) = 1$, and the structure factor $S(Q)$ describes the interactions between the particles. In the absence of interactions, like in a dilute solution, $S(Q) = 1$. So, from the scattered intensity $I(0)$, we can extract the mass of the particle in atomic units (MW, in g/mol), which coincides with the molecular mass if the particle consists of a single molecule, by introducing the concentration $c = n(MW/N_A)$ (g/cm^3) and the particle density $d = (MW/V_{part}.N_A)$ (g/cm^3) using the following equation:

$$MW = \frac{I(0)d^2N_A}{c\,\Delta\rho^2}, \qquad (4)$$

where N_A (mol^{-1}) is the Avogadro number and $\Delta\rho^2$ (cm^{-4}) the contrast.

Please cite this article in press as: Minić et al., Effect of Ligands on HP-Induced Unfolding and Oligomerization of β-Lactoglobulin, Biophysical Journal (2020), https://doi.org/10.1016/j.bpj.2020.10.019

Q8 ScÅtter software (http://www.bioisis.net/tutorial/9) was used to determine the intensity at zero angle $I(0)$ and the radius of gyration (R_g). These values are defined at small Q-values ($QR_g < 0.8$–1.4) by the Guinier approximation with (28)

$$\ln(I(Q)) = \ln(I(0)) - \frac{Q^2R_g^2}{3}. \quad (5)$$

We evaluated that, at the maximal QR_g-value of ~1.4, the deviation from the cylindrical form factor does not exceed ~2%. All the Guinier plots are shown in Figs. S5, S9, and S18. The distance distribution function $P(r)$ was calculated with PRIMUS (ATSAS) program (29).

The native BLG data were best fitted using the cylinder form factor model (28) in SasView software (https://www.sasview.org), which in particular fits the "bump" observed at high Q-values (Fig. S2, *C* and *D*). This form factor was therefore also chosen for the HP in situ experiments both at 30°C (Fig. S8, with χ^2-values obtained not exceeding ~1.2) and 37°C (Fig. S17). The SANS data measured after HP treatment for BLG oligomers were better fitted with a triaxial ellipsoid model (Figs. S6 *A* and S11 *A*; (30)), with χ^2-values given in Table 2.

BLG oligomers were also modeled by ab initio rigid-body modeling (in the Q-range: 0.009–0.5 $Å^{-1}$) using MASSHA software (ATSAS) (31); oligomers were built using BLG crystal structures from either monomers (3BLG.pdb) or dimers (1BEB.pdb) as starting building blocks. At a further step, because MASSHA can use only seven structures, we "manually" built linear BLG pentamers in MASSHA software. The previously best-fitted ellipsoid dimensions were taken into account to estimate the number and position of the different structures (monomers, dimers, or/and pentamers) (Fig. 6), which were further adjusted until a satisfactory fit regarding χ^2 (Table 2) and the error-weighted residual difference plots (Fig. S12).

We also performed ab initio modeling without making any assumption on BLG folding state using DAMMIF (32) or DAMMIN (33) software (ATSAS). Methods and results are described in the Supporting Materials and Methods, Figs. S13 and S14, and Table S2 for the simulation results.

RESULTS

Structural features for native and fully unfolded BLG

The sample details and the structural parameters obtained are summarized in Table S1. We checked that native BLG at pD 7.2 is dimeric by fitting SANS data with the theoretical curve obtained from the dimeric BLG crystal structure (1BEB.pdb (7)) using CRYSON software (ATSAS) (Fig. 2; (34)). In addition, using the experimental scattering length density of BLG determined by performing a "contrast variation" experiment (Table S1), we estimated, using Eq. 4 with $d = 1.35$ g/cm^3 and $c = 8$ mg/mL, that the apparent MW of the scattering particles is equal to 37,924 ± 1129 g/mol, in good agreement with the theoretical MW of dimeric BLG (37,142 g/mol). The pair-distribution function $P(r)$ analysis, giving a D_{max} of ~71 Å, confirms that the dimeric conformation of BLG is the most abundant one in our experimental conditions both at 8 mg/mL (Figs. 2 and S2 *B*) and 5 mg/mL protein (Fig. S2 *A*), using BLG crystal structures. Additionally, the best fit, using a cylinder form factor (Fig. S2, *C* and *D*), shows that the length of the cylinder is very similar to the length of the BLG dimer from the crystal structure: 75 ± 1 Å cylinder length compared with 73 ± 1 Å (PYMOL software), respectively, for native BLG at 8 mg/mL.

TABLE 1 Thermodynamic Parameters of Pressure Denaturation for BLG Samples Obtained from HP-UV/Vis Absorption Spectroscopy at 30 and 37°C

Sample	Temperature (°C)	ΔV_u (mL/mol)	$P_{1/2}$ (MPa)
BLG	30	−103 ± 8	168 ± 3
	37	−98 ± 6	170 ± 3
BLG-retinol	30	−158 ± 9	239 ± 1
	37	−191 ± 15	249 ± 2
BLG-resveratrol	30	−114 ± 8	180 ± 2

The presence of deuterated 6 M guanidine (Gdn)-DCl completely unfolds BLG, as shown by the SANS data that fit the Gaussian coil model commonly used for fully unfolded proteins (Fig. S3 *A*; (35)). The radius of gyration (R_g) increases from 23.5 ± 1.2 Å for native BLG to 41 ± 4 Å for the fully chemically unfolded protein. The bell-shaped plot in the Kratky representation confirms the well-folded and compact state of native BLG, whereas a "plateau" characteristic of Gaussian chains is observed in the presence of Gdn-DCl (Fig. S3 *B*). In native conditions, BLG-retinol and BLG-resveratrol complexes are superimposed to the curves of BLG without ligand (Fig. S4).

Effect of HP on BLG structure

SANS and UV/vis absorption spectroscopy measurements were performed by applying in situ HP up to ~300 MPa on BLG without ligand compared with BLG-retinol and BLG-resveratrol complexes.

For BLG without ligand and both BLG-ligand complexes, no significant change in the protein three-dimensional (3D) conformation is observed by HP-SANS up to ~150 MPa, whether for retinol (Fig. 3) or for resveratrol (Fig. S6). For such pressures, R_g-values (Fig. 4, *B* and *D*), obtained from the Guinier plots (Fig. S9), as well as the length and radius parameters extracted from the cylinder model used to fit SANS data (Figs. 4, *A* and *C* and S8) are similar compared to those obtained at the atmospheric pressure. Values of $I_{Q\to 0}$, reflecting protein MW and hydration-dependent contrast value (see Eq. 4), decrease very slightly with pressure (Fig. S7).

At higher pressures (above 150 MPa), two different transitions are observed according to protein concentration. At 5 mg/mL (Fig. 3, *A* and *B*), BLG starts to unfold continuously from ~200 MPa to reach a Gaussian chain conformation at ~300 MPa, without any significant change in the size of the dimeric protein. This is clearly observed in the Kratky representation with a transition from bell-shaped curves, without any change in the Q-position of the peak, to a "plateau," characteristic of curves with Q^{-2} variation (Fig. 3 *B*). BLG conformational changes are highlighted by both higher $I_{Q\to 0}$ (Fig. S7 *A*) and R_g (Fig. 4 *B*) to values up to ~40 Å, found for the fully chemically unfolded protein. In contrast,

Please cite this article in press as: Minić et al., Effect of Ligands on HP-Induced Unfolding and Oligomerization of β-Lactoglobulin, Biophysical Journal (2020), https://doi.org/10.1016/j.bpj.2020.10.019

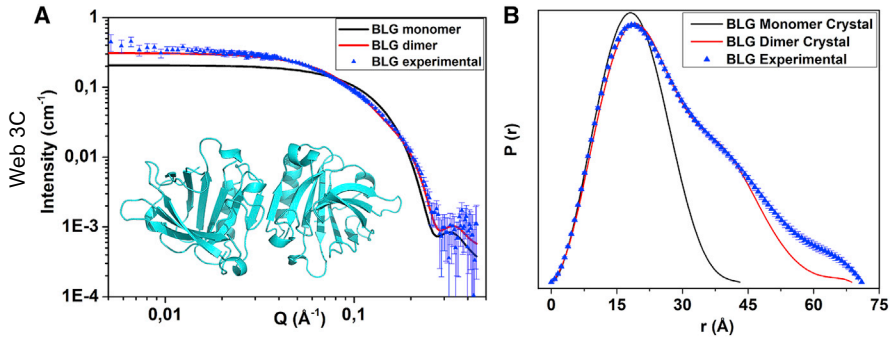

FIGURE 2 (*A*) SANS intensities of BLG (8 mg/mL) in 50 mM Tris D_2O buffer at pD 7.2. The full red and dotted black lines correspond to the theoretical curves calculated from BLG dimer (1BEB.pdb) or monomer (3BLG.pdb) crystal structure files, respectively, using CRYSON software. The inset is a representation of the BLG dimer (1BEB.pdb). (*B*) The pair-distribution function *P*(r) analysis with the same curve code, showing a D_{max} of ~71 Å for BLG dimer, is given. To see this figure in color, go online.

at 8 mg/mL, BLG unfolding from ~200 MPa is not complete and still exhibits bell-shaped curves in the Kratky representation (Fig. S6 *B*). At that concentration, we observe a transition from a globular state to a larger one, as shown by the shift of the curve peak to lower *Q*-values (Fig. S6 *B*). BLG oligomerizes from the native dimer observed up to ~150 MPa to a tetrameric conformation at ~250–300 MPa, as shown by the doubled $I_{Q\to 0}$-value (Fig. S7 *B*), as well as higher R_g (Fig. 4 *D*). For both 5 and 8 mg/mL, the SANS curves are virtually superimposed up to ~150 MPa, as well as at ~250–300 MPa, whereas in between, the curves at ~200 MPa may illustrate the coexistence of two protein populations (Figs. 3 and S6). SANS curves can be fitted by a cylinder form factor up to ~150 MPa (Figs. 4, *A* and *C* and S8). At ~200–250 MPa, this model still fits the data, but such a fitting appears trickier, especially at 5 mg/mL, for which BLG tends to a Gaussian polymer chain (Fig. S8). At ~300 MPa, the cylinder model used as a form factor does not fit the data anymore at both BLG concentrations.

Effect of ligands on HP-induced structural changes of BLG

Retinol, which binds with high affinity to BLG hydrophobic cavity (4), shifts the onset of the pressure unfolding by ~50 MPa (Fig. 3, *C* and *D*). From ~200 MPa, the length and radius of the cylinder form factor, R_g, and $I_{Q\to 0}$ are reduced by ~20% compared to BLG without ligand (Figs. 4, *A* and *B* and S7 *A*). Above ~200 MPa, the BLG-retinol complex starts to unfold and shows a large increase of the cylinder length and radius parameters, R_g, and $I_{Q\to 0}$, approaching the values found for BLG without ligand at ~300 MPa (Figs. 4, *A* and *B* and S7 *A*).

In contrast, resveratrol, with low affinity to BLG surface site(s) (5,36), does not induce any significant change of the structural features reported above for BLG without ligand from in situ HP-SANS (Fig. S6). However, the transition with pressure described for BLG without ligand at 8 mg/mL appears slightly more "abrupt" in the presence

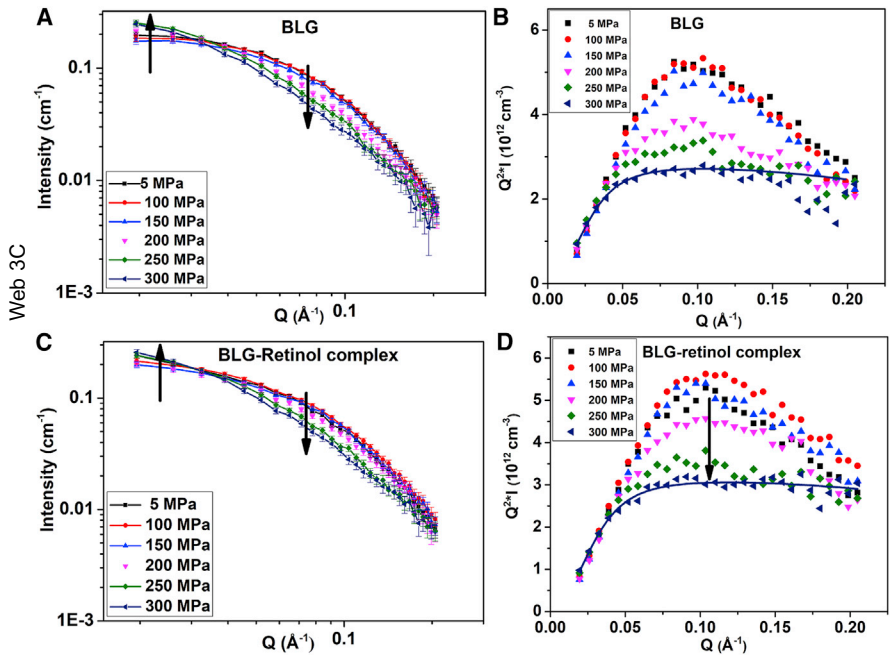

FIGURE 3 (*A* and *C*) In situ HP-SANS intensities of BLG (5 mg/mL (pD 7.2), 30°C) in the absence or presence of retinol at different pressures. The arrows represent the directions of SANS intensity changes with increasing pressure. Full lines are guides for the eyes. (*B* and *D*) The same data are shown in the Kratky representation. The dark blue full lines represent the fits obtained at ~300 MPa, with the "plateau" characteristic of a Gaussian chain conformation. For BLG without ligand, fitting has been performed up to ~0.12 Å because of noisy data at higher *Q*-values. To see this figure in color, go online.

Please cite this article in press as: Minić et al., Effect of Ligands on HP-Induced Unfolding and Oligomerization of β-Lactoglobulin, Biophysical Journal (2020), https://doi.org/10.1016/j.bpj.2020.10.019

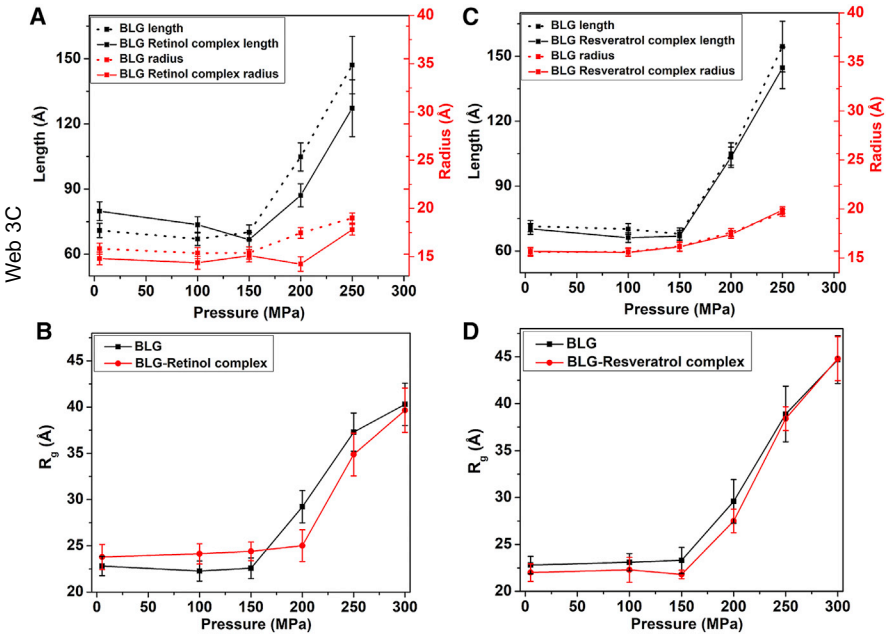

FIGURE 4 Effects of ligand binding on HP-induced 3D conformational and Trp local unfolding of BLG at 30°C. (*A* and *C*) Evolution is shown as a function of pressure of the cylinder length and radius obtained from the analytical model that fits HP-SANS data, in the absence or presence of (*A*) retinol (5 mg/mL BLG) or (*C*) resveratrol (8 mg/mL BLG). At ∼300 MPa, the virtually fully unfolded protein cannot be fitted by a cylinder form factor anymore. (*B* and *D*) Dependence is shown as a function of pressure of the radius of gyration obtained from HP-SANS data in the absence or presence of (*B*) retinol (5 mg/mL BLG) or (*D*) resveratrol (8 mg/mL BLG). To see this figure in color, go online.

of resveratrol, with two well-marked protein states, one up to ∼150 MPa and the other at ∼250–300 MPa, with a transitory state at ∼200 MPa (Fig. S6 *D*).

In the HP-UV/vis absorption study, using the fourth derivative mode, BLG spectra exhibit absorbance maxima at 276, 291, and 284 nm, corresponding to tyrosine (Tyr) or Trp residues or both of them, respectively (Figs. 5, *A* and *B* and S10). For all BLG samples, HP treatment induces a "blue shift" of these maxima, especially of the Trp-dependent peak, toward lower wavelengths, indicating local unfolding of the protein (Figs. 5 and S10; (11)).

The denaturation curves are well fitted by Eq. 2 (Fig. 5, *C* and *D*) but, because BLG HP denaturation is a pseudoequilibrium (because of irreversible reactions; see below), the only thermodynamic parameters we extracted are the unfolding volume change (ΔV_u) and the value of the half-denaturation pressure ($P_{1/2}$) (Table 1). In agreement with HP-SANS, the UV/vis absorption measurements confirm that retinol strongly stabilizes BLG during HP denaturation, with a shift in the change of the Trp local structure of ∼100 MPa (Fig. 5, *B* and *C*) and a significant increased transition pressure ($P_{1/2}$) of ∼70 MPa in the presence of the ligand (Fig. 5 *C*; Table 1). In contrast, resveratrol has virtually no effect on the stability of the local Trp environment of BLG as measured by UV/vis absorption (Figs. 5 *D* and S10; Table 1). The deduced ΔV_u shows that retinol, but not resveratrol, induces a larger volume change during BLG unfolding, as compared with BLG without ligand (Table 1).

We can therefore conclude that during in situ HP denaturation of BLG, retinol, which has a high-affinity binding to the BLG cavity, is able to partly but significantly prevent BLG unfolding, both at the local Trp environment and at the protein three-dimensional conformation. On the contrary, resveratrol, which binds with low-affinity protein surface site(s), has no significant effect on BLG unfolding.

BLG irreversible refolding and oligomerization

First, we compare unliganded BLG. To account for concentration effects (5 or 8 mg/mL), SANS data were normalized to protein concentration (Figs. 6 *A* and S11 *A*). After HP treatment up to ∼300 MPa, return to atmospheric pressure enables BLG to refold, but only partially. At 5 mg/mL, BLG without ligand, although completely unfolded at ∼300 MPa (Fig. 3 *B*), is partially refolded at atmospheric pressure, as evidenced by the bell-shaped SANS curves in the Kratky representation, characteristic of globular particles (Fig. 6 *A*). As mentioned before, a higher BLG concentration prevents the complete unfolding of the protein, but it may also favor protein partial refolding, as shown by the increased intensity of the peak at 8 compared to 5 mg/mL (Fig. 6 *A*). UV/vis absorption spectroscopy confirms that HP induces irreversible structural local changes, with only ∼50% recovery compared to the native protein when pressure returns to atmospheric value (Figs. 5 *A* and S10 *A*).

Interestingly, HP treatment back and forth up to ∼300 MPa causes also irreversible oligomerization, as observed for BLG without ligand at 8 mg/mL, with a large increase of both $I_{Q\to 0}$ (from 0.37 to 2.9 cm^{-1}) and R_g (from 23.5 to 70.5 Å) (Fig. 6 *A*). We use the term "oligomerization" instead of "aggregation" because the larger objects we observed exhibit a finite size, at least in the SANS *Q*-range we used. *I*(*Q*) spectra of samples after HP treatment exhibit a well-defined plateau in the Guinier *Q*-range

Please cite this article in press as: Minić et al., Effect of Ligands on HP-Induced Unfolding and Oligomerization of β-Lactoglobulin, Biophysical Journal (2020), https://doi.org/10.1016/j.bpj.2020.10.019

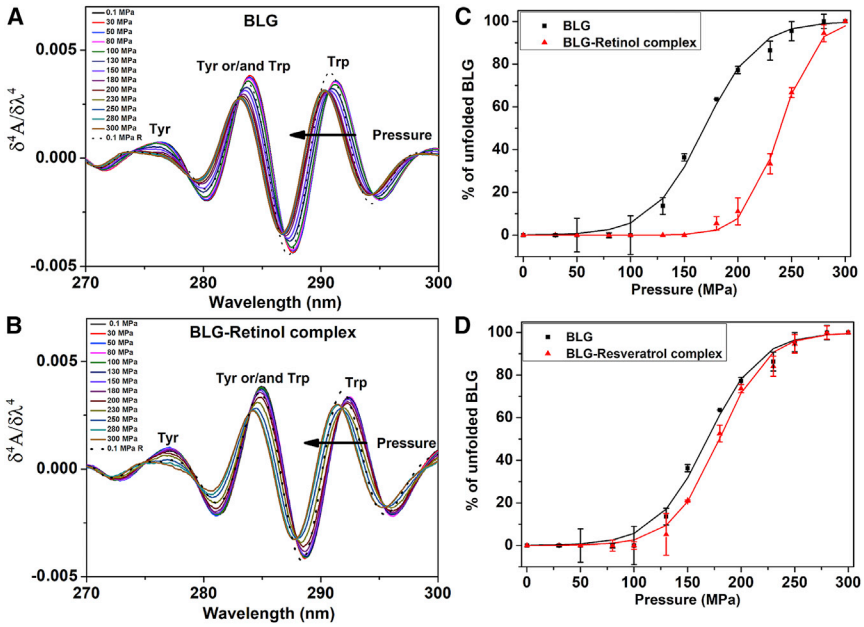

FIGURE 5 (*A* and *B*) Fourth derivative of in situ HP-UV/vis absorption spectra of BLG (2 mg/mL (pH 7.2), 30°C) as a function of pressure in (*A*) the absence or (*B*) the presence of retinol (1:1 protein/ligand molar ratio). "0.1 MPa R" is the curve obtained by decreasing back the pressure to 0.1 MPa after ~300 MPa treatment. (*C* and *D*) Percentage of unfolded BLG (Eq. 1) and the corresponding unfolding fits (*full lines*, Eq. 2) are shown as a function of pressure in the absence or presence of (*C*) retinol or (*D*) resveratrol, obtained from the fourth derivative mode of absorption spectra. To see this figure in color, go online.

(Fig. S11 *A*), in contrast to the huge low-Q increase observed for the same samples during thermal denaturation, which is the sign of large aggregation (data not shown). Moreover, according to MASSHA software and ellipsoid fitting, the oligomers do not exceed the size of 18 BLG monomers (Table 2). SDS-PAGE data show that covalent bonds significantly contribute to BLG oligomerization even if we cannot exclude other types of intermolecular interactions (Fig. 7).

At 5 mg/mL, compared to native BLG, the SANS curve after HP treatment is shifted to lower Q-values in the Kratky representation (from ~0.1 to ~0.04 $Å^{-1}$), which is characteristic of larger scattering objects (Fig. 6 *A*). At 8 mg/mL, the larger size (compared to native protein) of BLG without ligand observed in situ at ~300 MPa (Fig. S6 *B*) is also increased when pressure returns to 1 bar, as shown by the peak shift from ~0.055 $Å^{-1}$ (Fig. S6 *B*) to ~0.03 $Å^{-1}$ (Fig. 6 *A*).

The ab initio envelopes of BLG oligomers obtained after HP treatment simulated by MASSHA (31), DAMMIN (33), and DAMMIF (32) show that a higher protein concentration induces larger oligomers, which confirms the increased dimensions of the ellipsoid model that fits the data in SasView (Fig. 6, *B* and *D*; Table 2). MASSHA simulations use BLG crystal structures (monomers or dimers) as building blocks that are assumed to remain "folded." However, without making any assumption on BLG folding state, both DAMMIF (32) and DAMMIN (33) ab initio simulations confirm the MASSHA results (Figs. S13 and S14, *B* and *D*; Tables 2 and S2). Although DAMMIN simulations are known to be more accurate for extended structures such as BLG oligomers than DAMMIF ones, results obtained from the two methods are roughly comparable (Figs. S13 and S14; Table S2).

Effect of ligands on BLG refolding and oligomerization

Resveratrol binding does not significantly change HP-induced BLG refolding and oligomerization (Fig. 6 *A*). In contrast, retinol binding partly, but significantly, prevents both protein irreversible unfolding and oligomerization extent, as observed with the peak shift to a lower Q-value (0.06 $Å^{-1}$) compared to BLG without ligand (0.04 $Å^{-1}$)

TABLE 2 Fitting of SANS Data from BLG Samples after HP Treatment Using Triaxial Ellipsoid or Rigid-Body Modeling

	Ellipsoid Fitting				Rigid-Body Modeling		
Sample	*a* (Å)	*b* (Å)	*c* (Å)	χ^2	Number of BLG Monomers	MW_{app} (kDa)	χ^2
BLG (5 mg/mL)	12.8	55.0	115.5	0.73	11	204.1	1.20
BLG-retinol (5 mg/mL)	8.1	35.0	163.5	0.99	8	148.4	1.45
BLG (8 mg/mL)	13.4	74.4	108.9	1.68	18	333.9	1.29
BLG-resveratrol (8 mg/mL)	14.0	79.3	105.8	2.52	18	333.9	1.73

a, *b*, and *c* represent minor, polar, and major equatorial radii, respectively. Triaxial ellipsoid modeling performed in SasView; rigid-body modeling performed in MASSHA (ATSAS).

Please cite this article in press as: Minić et al., Effect of Ligands on HP-Induced Unfolding and Oligomerization of β-Lactoglobulin, Biophysical Journal (2020), https://doi.org/10.1016/j.bpj.2020.10.019

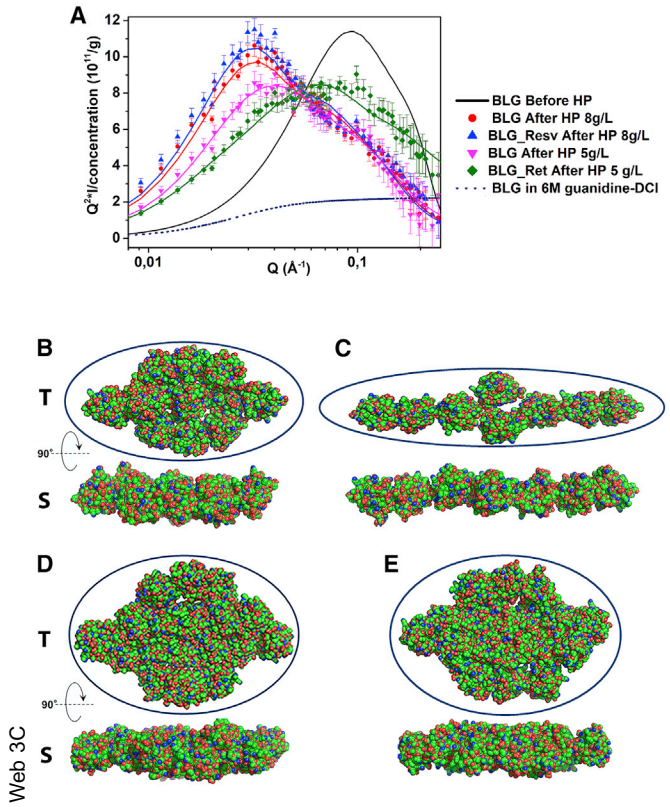

FIGURE 6 (*A*) Kratky representation (but with the *x* axis in log) of BLG SANS intensities measured, at pD 7.2, in quartz Hellma cells after ~300 MPa HP treatment and normalized to BLG concentration. Black full and dotted lines are for native or fully chemically unfolded BLG (by deuterated 6 M Gdn-DCl), respectively (8 mg/mL). The other curves represent BLG without ligand at 5 (*upside-down solid pink triangle*) or 8 mg/mL (*solid red circle*), BLG-retinol at 5 mg/mL (*solid green diamond*), and BLG-resveratrol at 8 mg/mL (*solid blue triangle*). The corresponding colored full lines represent the best fits by the ellipsoid analytical model in SasView program. (*B–E*) Ab initio shapes of BLG oligomers corresponding to MASSHA models obtained with the smallest χ^2 are shown (Table 2). (*B* and *D*) BLG without ligand at 5 or 8 mg/mL, respectively, (*C*) BLG-retinol (5 mg/mL), and (*E*) BLG-resveratrol (8 mg/mL) are shown. *T* and *S* denote top and side views, respectively. Green, blue, and red spheres represent carbon, nitrogen, and oxygen atoms, respectively. SasView ellipsoid shapes are superimposed to MASSHA model buildings. To see this figure in color, go online.

(Fig. 6 *A*). However, the BLG-retinol complex remains significantly different compared to the native dimeric BLG, meaning that HP treatment is not reversible even in the presence of retinol.

MASSHA ab initio simulations show that retinol binding reduces the average size of BLG oligomers that are less dense and more elongated compared to BLG without ligand (Fig. 6, *B* and *C*; Table 2). DAMMIF and DAMMIN simulations confirm that BLG-retinol oligomers exhibit a more linear shape with a smaller density of "beads" (Figs. S13 and S14, *B* and *C*; Table S2). In contrast, resveratrol binding does not significantly modify oligomer envelopes obtained by MASSHA (Fig. 6, *D* and *E*), DAMMIF (Fig. S13, *D* and *E*), or DAMMIN (Fig. S14, *D* and *E*).

SDS-PAGE in nonreducing conditions shows that at least one part of HP-induced irreversible oligomerization is covalent in all BLG samples, with the presence of not only covalent dimers but also higher *MW* covalent oligomers (Fig. 7 *A*). A higher BLG concentration induces higher *MW* oligomers in nonreducing SDS-PAGE (Fig. 7 *B*). Resveratrol binding does not significantly decrease the number of high *MW* oligomers, whereas retinol decreases the number of both covalent dimers and higher *MW* oligomers, resulting in a higher number of preserved monomers (Fig. 7).

Temperature effect on BLG structural changes

Because temperature is known to emphasize hydrophobic effects, retinol binding effect on BLG was also measured at 37°C to compare with 30°C (Fig. S15). We found that such a temperature increase strengthens the effect of retinol to prevent HP-induced BLG changes. At ~200 MPa, we observe a reduction of 8.4 Å of the radius of gyration for the BLG-retinol complex compared to that of BLG without ligand, whereas this reduction is only 4.2 Å at 30°C at the same pressure (Figs. 4 *B* and S16 *A*), as clearly illustrated in the Kratky representation (Fig. 3, *B* and *D* compared with Fig. S15, *C* and *D*). At ~200 MPa, BLG without ligand is much more unfolded by HP at 37°C than at 30°C (Fig. S15 *E*), whereas the effect of retinol on the stabilization of the BLG-retinol complex folding is emphasized by temperature (Fig. S15 *F*). In situ HP-UV/vis absorption confirms this strengthened effect of retinol on BLG stabilization at higher temperature. Indeed, $P_{1/2}$ increases significantly from 239 ± 1 MPa at 30°C to 249 ± 2 MPa at 37°C, and the volume reduction is more pronounced, with ΔV_u decreasing from −158 ± 9 at 30°C to −191 ± 15 mL/mol at 37°C (Fig. 5 *C* compared with Fig. S19; Table 1). In contrast, a temperature increase from 30 to 37°C has no significant effect on both $P_{1/2}$ and ΔV_u for BLG without ligand (Table 1).

The unexpected decreased $I_{Q\to 0}$ observed upon in situ HP denaturation for BLG without ligand at 37°C (Fig. S16 *B*), whereas at 30°C $I_{Q\to 0}$ increases (Fig. S7 *A*), may be due to the limited accessible low *Q*-range in an HP cell that prevents to observe large size objects. However, using a larger *Q*-range as in a quartz cell, on return to ambient pressure after ~300 MPa treatment, SANS measurements show that temperature has no or little influence on the aggregated BLG structures (Fig. S11 *B*).

DISCUSSION

In our study, we combined in situ HP-SANS and HP-UV/vis absorption spectroscopy in an original way to probe the mechanisms of ligand effect on the denaturation of BLG by pressure. We report that retinol, which binds the BLG cavity with high affinity (6), prevents protein unfolding both at 3D and local structural levels and reduces its

Please cite this article in press as: Minić et al., Effect of Ligands on HP-Induced Unfolding and Oligomerization of β-Lactoglobulin, Biophysical Journal (2020), https://doi.org/10.1016/j.bpj.2020.10.019

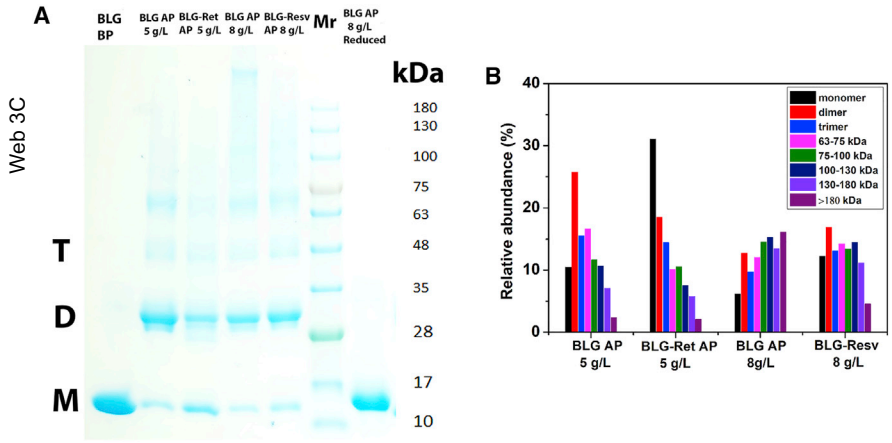

FIGURE 7 (*A*) SDS-PAGE (4–20% polyacrylamide gel) of BLG samples after HP treatment at ∼300 MPa. (*Wells from left to right side*) BLG without ligand before HP, HP-treated BLG without ligand (5 mg/mL), HP-treated BLG-retinol (5 mg/mL), HP-treated BLG (8 mg/mL), HP-treated BLG-resveratrol (8 mg/mL), and HP-treated BLG in reducing conditions (with 5% β-mercaptoethanol) are shown, showing the reduction of covalent disulfide bonds. *M*, *D*, and *T* denote BLG monomers, dimers, and trimers, respectively. *MW* markers (*Mr*) with the corresponding values in kDa are indicated. (*B*) Relative intensities of the protein bands corresponding to the different *MW* of BLG oligomers are shown. To see this figure in color, go online.

oligomerization when back to the atmospheric pressure. In contrast, resveratrol, known to bind with a lower affinity on different BLG surface site(s) (9,36), has virtually no significant effect on BLG structural changes.

Depending on pH, temperature, and concentration conditions, BLG adopts various assembly conformations, i.e., monomer, dimer, or octamer structures (16). We checked that, at neutral pH, native BLG is mostly a dimer, whereas the presence of Gdn-DCl, induces its complete unfolding (Figs. 2 and S2), in agreement with structural features observed by SAXS (37). The scattering intensity upturn observed at low Q-values in Fig. 2 *A* is probably due to the presence of a very small number of larger BLG oligomers than dimers (mostly octamers) (16,18). A very small number of larger oligomers (estimated to be ∼3% in volume) could explain such an upturn of intensity and the slight difference between the apparent *MW* found in this study, other ones reported in similar conditions (38), and the theoretical one. Note that the D_{max}-value of ∼71 Å is, however, similar to what was published before (38) for the dimeric conformation of BLG (Fig. 2 *B*).

In situ HP-SANS is a powerful tool to probe BLG 3D conformational subtle changes upon pressure increase. No significant change in the structure of BLG is observed up to ∼150 MPa except a slight decrease of $I_{Q\to 0}$, probably due to both BLG partial dissociation of native dimers into monomers, as similarly observed both by HP-SAXS (13) and HP-SANS (39,40) under moderately high pressures, and an increase of protein hydration, which reduces the contrast of BLG in D_2O. The UV/vis absorption "blue" shift upon pressure, highlighted by spectra fourth derivatives (Figs. 5 and S10), indicates a higher polarity of Trp environment as a consequence of the movement of the aromatic side chains from the protein hydrophobic environment toward a more hydrated BLG cavity during protein unfolding (11). In particular, the Trp19 residue, buried into the hydrophobic cavity of BLG in native condition (Fig. 1), can be exposed to solvent upon denaturation (41).

At 5 mg protein/mL, from ∼200 up to ∼300 MPa, pressure induces a strong decrease of BLG compactness (Fig. 3, *B* and *D*), the continuously reduced SANS intensity probably being due to a higher hydration of the protein arising from both protein unfolding and water penetration inside BLG cavity (39). At this concentration, BLG is completely unfolded at ∼300 MPa into a Gaussian chain. The free reactive Cys121 (Fig. 1), not accessible in native folded BLG, can indeed form intermolecular disulfide bridges when exposed to the solvent by protein unfolding and also exchange with the disulfide bonds already present in the native state (42).

A higher protein concentration (8 mg/mL) partially preserves BLG from a complete unfolding, as already reported by SAXS and SANS (39), by oligomerization of the native dimers to form tetramers at ∼250–300 MPa (Fig. S6). This pair association may not be due to steric (hindrance) effect, but rather to disulfide bond formations, as mentioned above. Indeed, at that protein concentration, the average distance between particles (dimers) can be estimated to be ∼200 Å, which is higher than the total length of the unfolded protein that is ∼150 Å (Fig. 4 *C*).

The high-affinity binding of retinol to the BLG cavity enables the ligand to significantly stabilize the protein both at tridimensional level (Figs. 3 and 4) and locally at Trp environment (Fig. 5). This is in agreement with a previous study showing that ligand binding to protein cavities increases pressure stability through a higher protein compaction (43). A previous HP-fluorescence study showed similar starting pressure points of unfolding for both BLG without ligand and the BLG-retinol complex, although this method does not probe directly retinol effects on protein Trp residues, but rather retinol fluorescence itself (12). These authors also highlight that retinol dissociates completely from BLG at ∼300 MPa (12), in accordance with our SANS data showing the total loss of protein compacity at that pressure (Fig. 3 *D*).

Please cite this article in press as: Minić et al., Effect of Ligands on HP-Induced Unfolding and Oligomerization of β-Lactoglobulin, Biophysical Journal (2020), https://doi.org/10.1016/j.bpj.2020.10.019

Because BLG denaturation by HP is a pseudoequilibrium in favor of the unfolded state of the protein, the unfolding volume change ΔV_u we calculated is not the apparent ΔV^0 usually deduced from equilibrium reactions. However, ΔV_u is very useful for estimating both conformational transitions and protein-solvent interactions. At the concentration of 2 mg/mL used in these HP-UV/vis measurements, protein oligomerization is very slow, as observed at 5 mg/mL by in situ HP-SANS (Fig. 3). Therefore, we focus instead, by UV/vis absorption spectroscopy, on BLG unfolding and ligand dissociation.

The volume change (−103 mL/mol) we observe for BLG without ligand at pH 7.2 is roughly comparable with the volume change (−90 mL/mol) at pH 2 obtained by HP-NMR (14). However, this slight difference can be assigned to a reduced resistance of BLG to pressure-induced conformational changes at neutral compared to acidic pH (12).

Apparent ΔV^0 is made up of three terms: 1) the constitutive volume of atoms, which remains unchanged at the pressures we used; 2) the hydration volume taking into account protein-solvent interactions; and 3) the cavity volume related to protein conformational changes. This third term is mainly responsible for the negative volume changes induced by HP. For all samples, the calculated ΔV_u are strongly negative, as reported before (2), probably indicating two phenomena: first, an HP-induced increase of the hydration of BLG cavity because the interactions of water molecules with a hydrophobic environment occupy less volume than in bulk water (44–46). The "blue" shift of Trp maximal absorption we observe under HP is compatible with the polarity change of the cavity due to the presence of water binding (Figs. 5 and S10); and second, the electrostriction of water molecules that may interact with the negative charges of BLG residues exposed to the solvent by the protein unfolding (2).

Retinol binding strengthens these observations (relative difference of ∼55 mL/mol compared to BLG without ligand; Table 1), suggesting that HP-induced unfolding of BLG presumably dissociates retinol binding from the hydrophobic cavity with the resulting entry of water molecules inside the hydrophobic pocket, as for the protein without ligand. In the case of resveratrol binding, there is a very small negative increase of the volume compared to BLG without ligand (relative difference of ∼11 mL/mol; Table 1) because the ligand binding on the BLG surface does not change significantly cavity hydration. Actually, the slight negative increase of ΔV_u, as compared with that of BLG without ligand, may be interpreted as an additional pressure effect on the hydration of the buried surface of the BLG-resveratrol complex after dissociation of the ligand (47).

The significant enhancement (in magnitude) of ΔV_u for BLG-ligand complexes, especially with retinol, upon pressure in comparison to BLG without ligand may also be explained by a larger initial volume of the complex at atmospheric pressure. Volume calculation of BLG crystal structures in the absence or presence of retinol or retinoic acid indeed showed a slightly larger volume (98 mL/mol) of BLG-ligand complexes in comparison with unliganded BLG (48). However, we have to keep in mind that 1) volumes calculated from crystal structures cannot be strictly compared to protein volumes in solution and 2) this increase represents less than 1% compared to the total protein volume, estimated from BLG crystal structure to be 13,000 mL/mol. This result that retinol binding into BLG cavity increases (in magnitude) the volume of the protein-ligand complex compared to the unliganded BLG may be counterintuitive. Our result is, however, in accordance with previous studies reporting the same observation for protein-ligand complexes with cavities as large as for BLG. For instance, heme binding to myoglobin is associated with a less compact volume of the complex and a higher volume change with pressure in the presence of the ligand, as reported by HP-circular dichroism (49). Similarly, ligand binding to cytochrome *P*-450 induces larger ΔV (in magnitude) measured by absorption during pressure denaturation (44).

In the BLG-*cis*-parinaric acid complex, the ligand, which exhibits a comparable affinity to that of retinol but for an outer hydrophobic binding site (not into the cavity), dissociates at lower pressure than the BLG-retinol complex (12). Therefore, ligand stabilization effects on BLG strongly depend on both ligand localization and affinity. BLG unfolding induces the movement of Trp19 from the buried hydrophobic cavity of the protein to solvent environment. Our result ($\Delta V_u = -98$ mL/mol) is in good agreement with the ΔV_u (−90 mL/mol) measured in BLG cavity by HP-NMR, yet measured at pH 2 (14). This is not surprising because Trp19 being noncharged, a pH change has no incidence on this amino acid, in contrast to amino acids such as Lys, as reported by NMR and SAXS with pressure (50).

BLG native folding is completely and irreversibly lost by pressures up to ∼300 MPa, whether in the absence or presence of ligand. The return to the atmospheric pressure does not enable to recover a complete folded state for BLG, but rather a "molten globule" state, as suggested by fluorescence and CD studies showing HP-induced formation of BLG molten globule with long term stability (41). Hence, it seems that an energy barrier between the BLG molten globule, stabilized by disulfide bonds, and the native protein cannot be overcome, even in the presence of retinol. The HP-induced BLG molten globule exhibits a cavity still able to bind various ligands but with different affinities in comparison to the native state, whereas HP treatment induces a decrease of retinol binding constant by a factor of two because of conformational changes of the hydrophobic cavity (51). A higher BLG concentration increases apparent R_g and the size of the scattering particles because of a larger extent of protein oligomerization promoted by HP (Fig. 4),

Please cite this article in press as: Minić et al., Effect of Ligands on HP-Induced Unfolding and Oligomerization of β-Lactoglobulin, Biophysical Journal (2020), https://doi.org/10.1016/j.bpj.2020.10.019

as already reported by chromatography (52). At 8 mg/mL, BLG structure is "preserved" from a complete unfolding by covalent oligomerization, in agreement with a study showing that thermal aggregation of BLG increases the content of ordered β-sheet secondary structures (53). Our SANS data clearly show that a higher protein concentration contributes to a larger stability of the BLG molten globule upon in situ HP treatment, probably because of a larger extent of protein covalent aggregation through nonnative disulfide bond exchange, as previously proposed for BLG under HP conditions (41).

HP treatment back and forth up to ~300 MPa produces irreversible oligomerization, as shown by SANS (Figs. 6 and S7) and nonreducing SDS-PAGE (Fig. 7). Similar results were reported by Patel et al. at pressures above ~200 MPa using two-dimensional PAGE method (54). Retinol reduces BLG oligomerization probably by a kinetic effect, whereas resveratrol has virtually no effect (Figs. 6, S13, and S14), in agreement with a previous study showing that binding to BLG of high-affinity ligands, such as fatty acids, could decrease the size of aggregates induced by heat or HP treatment (55). In retinol-induced stabilization of BLG folding, the protein may spend more time in its native conformation during in situ HP treatment, preventing SH group exposure to the solvent and consequently reducing the extent of aggregation through the formation of disulfide bridges.

Populating oligomers at pressures higher than ~150 MPa seems to violate the Le Chatelier principle, in contrast to the BLG dissociation from dimers into monomers we reported for pressures up to ~150 MPa (Fig. S7 *A*). The fact that our results appear not to be in accordance with the Le Chatelier principle can be explained by the chemical reactivity of BLG, which is not the same at ambient and high pressures. Above ~150 MPa, BLG monomers unfold, exposing free Cys residues to the solvent that are prone to covalent binding and protein oligomerization. The tetramers and/or larger oligomers obtained at these HP conditions are formed through irreversible disulfide bond exchanges and therefore are out of equilibrium.

SANS probes both covalent and noncovalent oligomers, giving access to their *MW* (Tables 2 and S2) and shapes (Figs. 6, S13, and S14) through analytical fitting and ab initio simulations. The MASSHA modeling uses the ellipsoid model parameters from SasView (Fig. 6) as constraints to "build" the oligomer shapes, in agreement with the data obtained on BLG oligomerization by γ irradiation (56). The overall envelopes are also consistent with those obtained from both DAMMIF and DAMMIN programs without any a priori geometrical assumption (Figs. S13 and S14; Table S2). Interestingly, we found for the BLG-retinol complex the formation of octamers in the presence of retinol (Table 2), as reported in other studies on BLG at pH 4–5 (18). Nonreducing SDS-PAGE gives access to only covalent oligomers, emphasizing the protective effect of retinol and the concentration influence on aggregation, at a qualitative way (Fig. 7 *A*). The relative intensities of the SDS-PAGE bands correspond to the different covalent oligomers in one sample and allow us to evaluate only qualitatively the *MW* of the sample (Fig. 7 *B*). Indeed, disulfide bonds make a significant contribution in BLG oligomerization, but noncovalent interactions cannot be excluded completely between monomers and/or oligomers. In addition, because the protein contrast at each pressure is unknown because of a higher protein hydration during unfolding, the apparent *MW* from SANS cannot be calculated from $I_{Q\to 0}$ and Eq. 4. So, it is difficult to compare *MW* deduced from SDS-PAGE and SANS experiments.

Although BLG has a relatively high thermal stability, with $T_{1/2}$ of ~70°C (57), HP-induced BLG unfolding is very sensitive to temperature. In particular, the effect of retinol is emphasized by temperature, known to foster hydrophobic interactions (58). For instance, retinol acetate binding to BLG is stimulated by temperature through rearrangements of the protein secondary structures and side chains interacting with the ligand (59). Our HP-SANS data indicate a higher stabilization effect of retinol at 37°C in comparison to 30°C, as observed for the apparent R_g (Figs. 4 *B* and S16 *A*) and the cylinder form factor parameters (Figs. 4 *A* and S16 *C*), showing that the BLG-retinol complex is more compact at 37 than 30°C (Fig. S15 *F*). The HP-UV/vis absorption study confirms these results, with a higher $P_{1/2}$ at 37 compared to 30°C (Figs. 5 *C* and S19).

As reported by molecular dynamics simulations (59), higher temperatures increase significantly the affinity of retinol for BLG and the stability of the BLG-retinol complex compared to BLG alone, through structural rearrangements in the BLG loop involved in the interaction with retinol. Therefore, these structural changes with temperature may induce a larger volume of the complex at ambient pressure and explain the higher ΔV_u (in amplitude) of the complex unfolding with HP compared to BLG alone (Table 1).

A higher temperature also promotes the hydrophobic aggregation of unfolded BLG induced by HP, producing large oligomers that may not be observed in the restricted *Q*-range of our HP cell, causing an apparent decreased $I_{Q\to 0}$ for BLG at 37°C (Fig. S16 *B*) contrary to measurements at 30°C (Fig. S7 *A*).

CONCLUSIONS

We report here the effects of two ligands, retinol and resveratrol, with different affinity and binding sites, on the pressure stability of BLG, the main whey protein, by combining in situ HP-SANS and HP-UV/vis absorption spectroscopy. Retinol, which binds the BLG cavity with high affinity, strongly stabilizes the protein upon HP. The pressure effect on the BLG-retinol complex leads to a more negative unfolding volume (ΔV_u) because of the

pressure-induced binding of water molecules inside the cavity, ligand dissociation, and mainly cavity volume change itself. Thus, this cavity volume is mainly responsible for the negative ΔV_u. In contrast, resveratrol, which has a low-affinity binding for BLG surface site(s), shows no significant effect on the stability of the protein but only a slight negative increase of ΔV_u compared to BLG without ligand. The return to atmospheric pressure after HP treatment up to ~300 MPa produces irreversible covalent oligomers of BLG, whose shape and size are reduced by retinol, but not resveratrol. More generally, our results highlight the mechanisms involved in the way ligands with high-affinity binding for internal hydrophobic cavities stabilize proteins like BLG, especially to resist pressure denaturation.

SUPPORTING MATERIAL

Supporting Material can be found online at https://doi.org/10.1016/j.bpj.2020.10.019.

AUTHOR CONTRIBUTIONS

S.M., C.L., A.B., and S.C. designed the study. S.M., B.A., A.H., C.L., A.B., and S.C. conducted and performed HP-SANS experiments. S.M., D.H., G.H.B.H., and S.C. conducted HP-UV/vis absorption spectroscopy. S.M., A.B., and S.C. analyzed and/or interpreted the data. S.M., A.B., and S.C. wrote the article.

ACKNOWLEDGMENTS

Q11 We thank Mikaela Börjesson (LLB, Saclay, France) for BLG preparation, as well as Adrien Lerbret (PAM, France), Marie-Sousai Appavou (JCNS, Germany), and Raphael Dos Santos Morais (LIBio, France) for their advice. The LLB neutron facility is acknowledged for beamtime on PACE SANS instrument.

SUPPORTING CITATIONS

References (60,61) appear in the Supporting Material.

REFERENCES

1. Silva, J. L., D. Foguel, and C. A. Royer. 2001. Pressure provides new insights into protein folding, dynamics and structure. *Trends Biochem. Sci.* 26:612–618.
2. Royer, C. A. 2002. Revisiting volume changes in pressure-induced protein unfolding. *Biochim. Biophys. Acta.* 1595:201–209.
3. Roche, J., J. A. Caro, …, C. A. Royer. 2012. Cavities determine the pressure unfolding of proteins. *Proc. Natl. Acad. Sci. USA.* 109:6945–6950.
4. Kontopidis, G., C. Holt, and L. Sawyer. 2002. The ligand-binding site of bovine beta-lactoglobulin: evidence for a function? *J. Mol. Biol.* 318:1043–1055.
5. Cheng, H., Z. Fang, …, L. Liang. 2018. Complexation of trans- and cis-resveratrol with bovine serum albumin, β-lactoglobulin or α-lactalbumin. *Food Hydrocoll.* 81:242–252.
6. Kontopidis, G., C. Holt, and L. Sawyer. 2004. Invited review: beta-lactoglobulin: binding properties, structure, and function. *J. Dairy Sci.* 87:785–796.
7. Brownlow, S., J. H. Morais Cabral, …, L. Sawyer. 1997. Bovine beta-lactoglobulin at 1.8 A resolution–still an enigmatic lipocalin. *Structure.* 5:481–495.
8. Knudsen, J. C., J. Otte, …, L. H. Skibsted. 2002. Effect of high hydrostatic pressure on the conformation of β-lactoglobulin A as assessed by proteolytic peptide profiling. *Int. Dairy J.* 12:791–803.
9. Liang, L., H. A. Tajmir-Riahi, and M. Subirade. 2008. Interaction of beta-lactoglobulin with resveratrol and its biological implications. *Biomacromolecules.* 9:50–56.
10. Dufour, E., M. C. Marden, and T. Haertlé. 1990. Beta-lactoglobulin binds retinol and protoporphyrin IX at two different binding sites. *FEBS Lett.* 277:223–226.
11. Kolakowski, P., E. Dumay, and J. Cheftel. 2001. Effects of high pressure and low temperature on β-lactoglobulin unfolding and aggregation. *Food Hydrocoll.* 15:215–232.
12. Dufour, E., G. H. Hoa, and T. Haertlé. 1994. High-pressure effects on beta-lactoglobulin interactions with ligands studied by fluorescence. *Biochim. Biophys. Acta.* 1206:166–172.
13. Panick, G., R. Malessa, and R. Winter. 1999. Differences between the pressure- and temperature-induced denaturation and aggregation of beta-lactoglobulin A, B, and AB monitored by FT-IR spectroscopy and small-angle X-ray scattering. *Biochemistry.* 38:6512–6519.
14. Kuwata, K., H. Li, …, K. Akasaka. 2001. High pressure NMR reveals a variety of fluctuating conformers in beta-lactoglobulin. *J. Mol. Biol.* 305:1073–1083.
15. Loupiac, C., M. Bonetti, …, P. Calmettes. 2006. Beta-lactoglobulin under high pressure studied by small-angle neutron scattering. *Biochim. Biophys. Acta.* 1764:211–216.
16. Mercadante, D., L. D. Melton, …, G. B. Jameson. 2012. Bovine β-lactoglobulin is dimeric under imitative physiological conditions: dissociation equilibrium and rate constants over the pH range of 2.5-7.5. *Biophys. J.* 103:303–312.
17. Celej, M. S., G. G. Montich, and G. D. Fidelio. 2003. Protein stability induced by ligand binding correlates with changes in protein flexibility. *Protein Sci.* 12:1496–1506.
18. Gottschalk, M., H. Nilsson, …, B. Halle. 2003. Protein self-association in solution: the bovine beta -lactoglobulin dimer and octamer. *Protein Sci.* 12:2404–2411.
19. Hamada, D., and C. M. Dobson. 2002. A kinetic study of beta-lactoglobulin amyloid fibril formation promoted by urea. *Protein Sci.* 11:2417–2426.
20. Fox, K. K., V. H. Holsinger, …, M. H. Pallansch. 1967. Separation of β-lactoglobulin from other milk serum proteins by trichloroacetic acid. *J. Dairy Sci.* 50:1363–1367.
21. Collini, M., L. D'Alfonso, and G. Baldini. 2000. New insight on beta-lactoglobulin binding sites by 1-anilinonaphthalene-8-sulfonate fluorescence decay. *Protein Sci.* 9:1968–1974.
22. Laemmli, U. K. 1970. Cleavage of structural proteins during the assembly of the head of bacteriophage T4. *Nature.* 227:680–685.
23. Hui Bon Hoa, G., P. Douzou, …, C. Balny. 1982. High-pressure spectrometry at subzero temperatures. *Anal. Biochem.* 120:125–135.
24. Lange, R., N. Bee, …, J. Frank. 1996. Fourth derivative UV-spectroscopy of proteins under high pressure II. Application to reversible structural changes. *Eur. Biophys. J.* 24:284–292.
25. Annighöfer, B., A. Hélary, …, S. Combet. 2019. A high pressure cell using metallic windows to investigate the structure of molecular solutions up to 600 MPa by small-angle neutron scattering. *Rev. Sci. Instrum.* 90:025106.
26. Brûlet, A., D. Lairez, …, J.-P. Cotton. 2007. Improvement of data treatment in small-angle neutron scattering. *J. Appl. Cryst.* 40:165–177.
27. Nikolaidis, A., M. Andreadis, and T. Moschakis. 2017. Effect of heat, pH, ultrasonication and ethanol on the denaturation of whey protein isolate using a newly developed approach in the analysis of difference-UV spectra. *Food Chem.* 232:425–433.
28. Guinier, A., and G. Fournet. 1955. Small Angle Scattering of X-Rays. John Wiley & Sons, Inc., New York.

Please cite this article in press as: Minić et al., Effect of Ligands on HP-Induced Unfolding and Oligomerization of β-Lactoglobulin, Biophysical Journal (2020), https://doi.org/10.1016/j.bpj.2020.10.019

29. Konarev, P. V., V. V. Volkov, …, D. I. Sverguna. 2003. PRIMUS: a windows PC-based system for small-angle scattering data analysis. *J. Appl. Cryst.* 36:1277–1282.

30. Feigin, L. A., and D. I. Svergun. 1987. Structure Analysis by Small-Angle X-Ray and Neutron Scattering. Plenum Press, New York.

31. Konarev, P. V., M. V. Petoukhova, and D. I. Sverguna. 2001. MASSHA-a graphics system for rigid-body modelling of macromolecular complexes against solution scattering data. *J. Appl. Cryst.* 34:527–532.

32. Franke, D., and D. I. Svergun. 2009. *DAMMIF*, a program for rapid *ab-initio* shape determination in small-angle scattering. *J. Appl. Cryst.* 42:342–346.

33. Svergun, D. I. 1999. Restoring low resolution structure of biological macromolecules from solution scattering using simulated annealing. *Biophys. J.* 76:2879–2886.

34. Svergun, D. I., S. Richard, …, G. Zaccai. 1998. Protein hydration in solution: experimental observation by x-ray and neutron scattering. *Proc. Natl. Acad. Sci. USA.* 95:2267–2272.

35. Calmettes, P., D. Durand, …, J. C. Smith. 1994. How random is a highly denatured protein? *Biophys. Chem.* 53:105–113.

36. Sahihi, M., Y. Ghayeb, and A. K. Bordbara. 2013. Interaction of β-lactoglobulin with resveratrol:molecular docking and molecular dynamics simulation studies. *Chem. Biochem. Eng. Q.* 27:417–422.

37. Semisotnov, G. V., H. Kihara, …, K. Kuwajima. 1996. Protein globularization during folding. A study by synchrotron small-angle X-ray scattering. *J. Mol. Biol.* 262:559–574.

38. Anghel, L., A. Rogachev, …, R. V. Erhan. 2019. β-Lactoglobulin associative interactions: a small-angle scattering study. *Eur. Biophys. J.* 48:285–295.

39. Russo, D., M. G. Ortore, …, A. Paciaroni. 2013. The impact of high hydrostatic pressure on structure and dynamics of β-lactoglobulin. *Biochim. Biophys. Acta.* 1830:4974–4980.

40. Ortore, M. G., F. Spinozzi, …, G. Onori. 2006. High pressure small-angle neutron scattering study of the aggregation state of β-lactoglobulin in water and in water/ethylene-glycol solutions. *Chem. Phys. Lett.* 418:342–346.

41. Yang, J., A. K. Dunker, …, B. G. Swanson. 2001. Beta-lactoglobulin molten globule induced by high pressure. *J. Agric. Food Chem.* 49:3236–3243.

42. Funtenberger, S., E. Dumay, and J. C. Cheftel. 1997. High pressure promotes β-lactoglobulin aggregation through SH/S-S interchange reactions. *J. Agric. Food Chem.* 45:912–921.

43. Toleikis, Z., P. Cimmperman, …, D. Matulis. 2011. Determination of the volume changes induced by ligand binding to heat shock protein 90 using high-pressure denaturation. *Anal. Biochem.* 413:171–178.

44. Di Primo, C., G. Hui Bon Hoa, …, S. G. Sligar. 1992. Heme-pocket-hydration change during the inactivation of cytochrome P-450camphor by hydrostatic pressure. *Eur. J. Biochem.* 209:583–588.

45. Hui Bon Hoa, G., M. A. McLean, and S. G. Sligar. 2002. High pressure, a tool for exploring heme protein active sites. *Biochim. Biophys. Acta.* 1595:297–308.

46. Rupley, J. A., and G. Careri. 1991. Protein hydration and function. *Adv. Protein Chem.* 41:37–172.

47. Kornblatt, J. A., G. H. B. Hoa, and G. Mauk. 1988. The effects of pressure on porphyrin c -cytochrome b_5 complex formation. *J. Am. Chem. Soc.* 110:5909–5911.

48. Chen, C. R., and G. I. Makhatadze. 2015. ProteinVolume: calculating molecular van der Waals and void volumes in proteins. *BMC Bioinformatics.* 16:101.

49. Lerch, M. T., J. Horwitz, …, W. L. Hubbell. 2013. Circular dichroism and site-directed spin labeling reveal structural and dynamical features of high-pressure states of myoglobin. *Proc. Natl. Acad. Sci. USA.* 110:E4714–E4722.

50. Kitahara, R., K. Hata, …, C. A. Royer. 2011. Structural plasticity of staphylococcal nuclease probed by perturbation with pressure and pH. *Proteins.* 79:1293–1305.

51. Yang, J., J. R. Powers, …, B. G. Swanson. 2003. Ligand and flavor binding functional properties of β-lactoglobulin in the molten globule state induced by high pressure. *J. Food Sci.* 68:445–452.

52. Dumay, E. M., M. T. Kalichevsky, and J. C. Cheftel. 1994. High-pressure unfolding and aggregation of β-lactoglobulin and the baroprotective effects of sucrose. *J. Agric. Food Chem.* 42:1861–1868.

53. Sawyer, W. H., R. S. Norton, …, G. H. McKenzie. 1971. Thermodenaturation of bovine -lactoglobulin. Kinetics and the introduction of -structure. *Biochim. Biophys. Acta.* 243:19–30.

54. Patel, H. A., H. Singh, …, L. K. Creamer. 2006. Effects of heat and high hydrostatic pressure treatments on disulfide bonding interchanges among the proteins in skim milk. *J. Agric. Food Chem.* 54:3409–3420.

55. Considine, T., H. A. Patel, …, L. K. Creamer. 2007. Influence of binding conjugated linoleic acid and myristic acid on the heat- and high-pressure-induced unfolding and aggregation of β-lactoglobulin B. *Food Chem.* 102:1270–1280.

56. Oliveira, C. L., L. de la Hoz, …, F. M. Netto. 2007. Effects of gamma radiation on beta-lactoglobulin: oligomerization and aggregation. *Biopolymers.* 85:284–294.

57. Puyol, P., M. D. Perez, …, M. Calvo. 1994. Effect of binding of retinol and palmitic acid to bovine *β*-lactoglobulin on its resistance to thermal denaturation. *J. Dairy Sci.* 77:1494–1502.

58. Skipper, N. T. 1993. Computer simulation of methane-water solutions. Evidence for a temperature-dependent hydrophobic attraction. *Chem. Phys. Lett.* 207:424–429.

59. Ciuciu, A.-M. S., I. Aprodu, …, N. Stănciuc. 2016. Thermally driven interactions between β-lactoglobulin and retinol acetate investigated by fluorescence spectroscopy and molecular modeling methods. *Dairy Sci. Technol.* 96:405–423.

60. Volkov, V. V., and D. I. Svergun. 2003. Uniqueness of ab-initio shape determination in small-angle scattering. *J. Appl. Cryst.* 36:860–864.

61. Tuukkanen, A. T., G. J. Kleywegt, and D. I. Svergun. 2016. Resolution of *ab initio* shapes determined from small-angle scattering. *IUCrJ.* 3:440–447.